Quaternary Research 75 (2011) 512–522

Contents lists available at ScienceDirect

Quaternary Research

journal homepage: www.elsevier.com/locate/yqres

Holocene East Asian monsoon variation inferred from species assemblage and shell chemistry of the ostracodes from Hulun Lake, Inner Mongolia

Dayou Zhai [a], Jule Xiao [a,*], Lang Zhou [a], Ruilin Wen [a], Zhigang Chang [a], Xu Wang [a], Xindi Jin [b], Qiqing Pang [c], Shigeru Itoh [d]

[a] Key Laboratory of Cenozoic Geology and Environment, Institute of Geology and Geophysics, Chinese Academy of Sciences, Beijing 100029, China
[b] State Key Laboratory of Lithospheric Evolution, Institute of Geology and Geophysics, Chinese Academy of Sciences, Beijing 100029, China
[c] College of Resources, Shijiazhuang University of Economics, Shijiazhuang 050031, China
[d] Paleo Labo Co., Ltd., Saitama 335-0016, Japan

ARTICLE INFO

Article history:
Received 30 August 2010
Available online 10 March 2011

Keywords:
Hulun Lake
Inner Mongolia
Ostracodes
Trace element
Stable isotope
East Asian monsoon
Holocene

ABSTRACT

A sediment core from Hulun Lake, Inner Mongolia was analyzed for species assemblages and shell chemistry of ostracodes to investigate changes in the hydrology and climate of the East Asian summer monsoon margin during the Holocene. *Darwinula stevensoni* was abundant, *Ilyocypris* spp. scarce, littoral ostracodes absent and Mg/Ca, Sr/Ca and $\delta^{18}O$ were low 11,100 to 8300 yr ago, indicating high lake levels and cool/fresh waters. *Darwinula stevensoni* declined largely, *Ilyocypris* spp. throve, littoral ostracodes were rare and chemical indicators remained in low values 8300 to 6200 yr ago, suggesting that the lake continued high stands but water became warm. The lake then contracted and water became cool/brackish 6200 to 4300 yr ago. Littoral ostracodes flourished 4300 to 3350 yr ago, marking the lowest lake levels of the entire Holocene. The lake level recovered and water salinity decreased 3350 to 1900 yr ago. From 1900 to 500 yr ago, the lake maintained the preceding status albeit lowered stands and increased salinities 1100 to 800 yr ago. During the recent 500 yr, the lake expanded and water salinity decreased. The data imply that the East Asian summer monsoon did not intensify until 8300 yr ago and weakened dramatically 4300 to 3350 yr ago.

Introduction

Ostracodes, micro-crustaceans with calcite valves, are widely distributed in lakes and leave the valves of different instars and adults in the sediments. Species assemblages of fossil ostracodes have been used in paleolimnological studies (Delorme, 1969; Holmes, 2001; Mischke and Wünnemann, 2006). The ostracode valve chemistry, on the other hand, is increasingly applied for reconstructing past variations in salinity and temperature of lake waters that are associated with changes in the regional environment (Chivas et al., 1986; Xia et al., 1997a; De Deckker et al., 1999; Holmes et al., 2007).

A number of brackish-water and salt lakes occur in northern China, in which ostracodes are abundant and their fossil shells are well preserved (Wang and Dou, 1998). Fossil ostracodes in these lakes should provide ideal materials for investigating the physical and chemical processes occurring in lakes, which are closely related to the environmental conditions regionally. Until recently, however, less attention was paid either to the species assemblage or to the shell chemistry of the ostracodes (Zhang et al., 1989; Mischke and Wünnemann, 2006; Holmes et al., 2007; Mischke et al., 2008; Van der Meeren et al., 2010; Wrozyna et al., 2010). In this study, we present data of species assemblages and shell chemistry of fossil ostracodes from a sediment core recovered in the central part of Hulun Lake in northeastern Inner Mongolia. The lake is located at the northern margin of the modern East Asian summer monsoon where the environment is particularly sensitive to the monsoon variation (Chinese Academy of Sciences, 1984; Zhang and Lin, 1985). Therefore, the high-quality, high-resolution ostracode record of Hulun Lake has great potential to reveal detailed changes in the intensity of the East Asian monsoon during the Holocene and improve our understanding of the mechanism responsible for the monsoon variation.

Study site

Hulun Lake (48°30.667′–49°20.667′ N, 117°0.167′–117°41.667′ E; Fig. 1) is an inland lake formed in a graben in the late Pliocene (Xu et al., 1989). It has an area of 2339 km^2 and a maximum water depth of 8 m when the lake level attains to the highest status at an elevation of 545.3 m a.s.l. (measurements in 1964 by Xu et al., 1989). Today, the lake is closed and the maximum water depth is 5 m (Fig. 1). Low mountains and hills of Mesozoic volcanic formations border the lake on the northwestern side and form a fault-scarp shoreline. Broad lacustrine and alluvial plains are present along the southern and eastern shores of the lake. The lake has a catchment of 37,214 km^2

* Corresponding author. Fax: +86 10 6201 0846.
E-mail address: jlxiao@mail.iggcas.ac.cn (J.L. Xiao).

0033-5894/$ – see front matter © 2011 University of Washington. Published by Elsevier Inc. All rights reserved.
doi:10.1016/j.yqres.2011.02.008

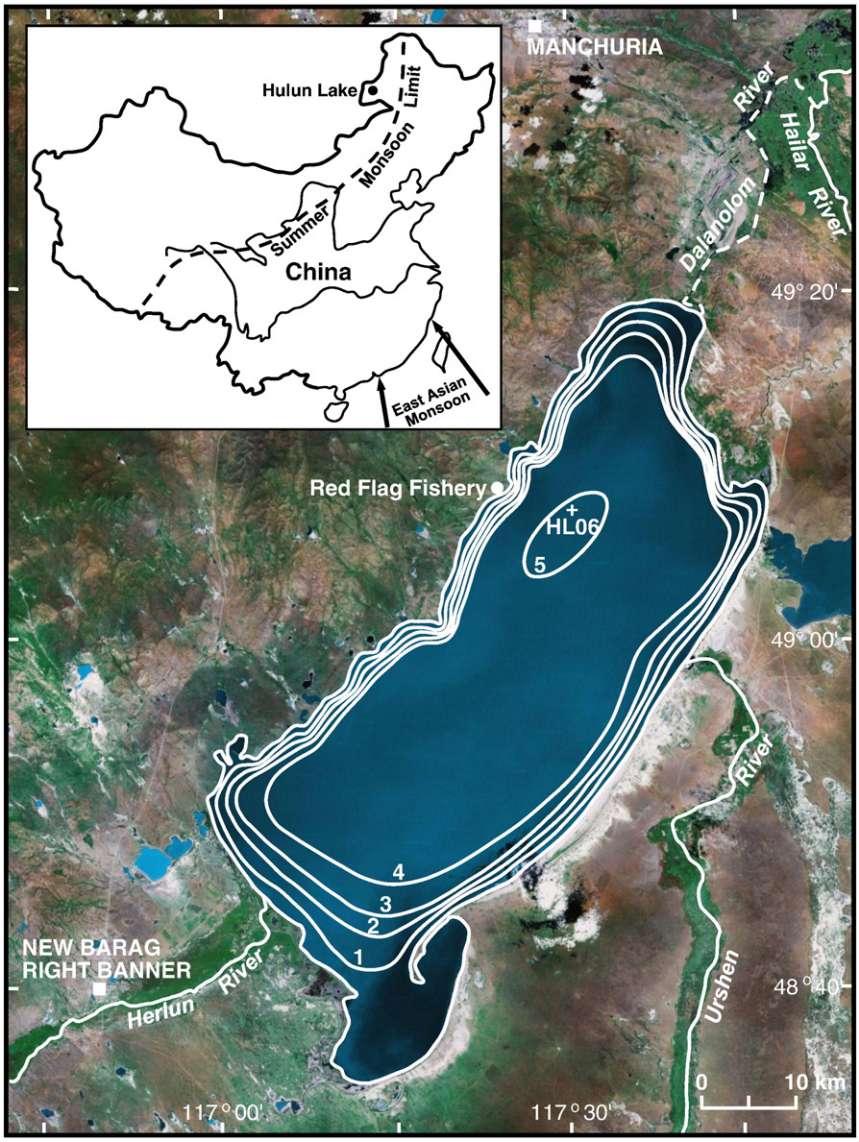

Figure 1. Map of Hulun Lake (from http://www.maps.google.com) showing the location of the HL06 sediment core. The bathymetric survey of the lake was conducted in July 2005 with a FE-606 Furuno Echo Sounder (contours in meters). In the inset, the current northern limit of the East Asian summer monsoon (dashed line) defined as the 400-mm isohyet of mean annual precipitation (Chinese Academy of Sciences, 1984) and the location of Hulun Lake (solid circle) are shown.

within the borders of China. Two major rivers, the Herlun and Ursheu River, enter the lake from the southwest and southeast. The Dalanolom River, an intermittent river to the northeast of the lake, drains the lake when the elevation of the lake level exceeds 543.4 m a.s.l. and enters the lake when the lake level is lower and the discharge of the Hailar River is larger as well (Xu et al., 1989; Fig. 1).

The lake is located in a semi-arid area, and the climate of the lake's region is under the influence of continental monsoon climate (Chinese Academy of Sciences, 1984; Xu et al., 1989). In the lake region, mean annual temperature is 0.3°C with a July average of 20.3°C and a January average of −21.2°C. Annual precipitation is 247–319 mm, and more than 80% of the annual precipitation falls in June–September. Annual evaporation reaches 1400–1900 mm, which is 5–6 times the annual precipitation. The lake is covered with ca. 1 m of ice from November to April.

The modern natural vegetation of the Hulun Lake basin is categorized as middle temperate steppe and dominated by grasses and *Artemisia* species (Compilatory Commission of Vegetation of China, 1980; Xu et al., 1989). The vegetation cover ranges from relatively moist forb–grass meadow–steppe in the piedmont belt to moderately dry grass steppe on the alluvial plain and dry bunchgrass–undershrub *Artemisia* steppe on the lacustrine plain. Halophilic Chenopodiaceae plants are developed in the lowlands. Small patches of open elm forests and sandy shrubs grow in the stabilized dune fields. Tall-grass meadows can be seen in the river valleys.

The water of Hulun Lake has a pH of 9.2 and a salinity of 2.5 g l^{-1} (measurements in 2009). The lake water contains major cations of Na^+ (81.9%), K^+ (1.8%), Mg^{2+} (13.7%), Ca^{2+} (2.6%) and Sr^{2+} (0.1%) and major anions of HCO_3^- (52.8%), CO_3^{2-} (9.4%), Cl^- (23.5%) and SO_4^{2-} (14.4%). Atomic ratios of Mg/Ca and Sr/Ca of the lake water are 8.8 and 0.02.

The ostracodes living in the lake today include *Limnocythere inopinata* (Baird), *Candoniella suzini* Schneider, *Pseudocandona albicans* (Brady), *Pseudocandona compressa* (Koch), *Cyclocypris serena* (Koch), *Ilyocypris gibba* (Ramdohr) and *Ilyocypris salebrosa* Stepanaiths (Xu et al., 1989; Wang and Ji, 1995). *Limnocythere inopinata* is the dominant species. Aquatic plants are scarce in the lake and confined to the areas of the river mouth and parts of the nearshore zone. The benthic fauna of the lake consists mainly of Oligochaeta, Mollusca, Hirudinea, Crustacea and Insecta, and these animals generally inhabit the northern part of the lake.

https://doi.org/10.1016/j.yqres.2011.02.008 Published online by Cambridge University Press

The lake region is sparsely populated. Local people are engaged in animal husbandry and fishery and do not undertake any agricultural activity. In 1948, the Inner Mongolian Fishery Company was set up to organize fishery production, and several fishery units had been formed along the lake during the subsequent decade. Fishery management activities have been carried out in winter since the 1990s to protect fish resources (Xu et al., 1989).

Material and methods

Sediment coring and sampling

Drilling was conducted at a water depth of 5 m in the central part of Hulun Lake in January 2006 when the lake was frozen (Fig. 1), using a Japanese-made TOHO drilling system (Model D1-B). A sediment core was extracted to a depth beneath the lake floor of 1.7 m and is designated HL06 (49°07.615′ N, 117°30.356′ E; Fig. 1). The core was collected in a polymethyl methacrylate tube using a piston corer. The core section was split, photographed and described on site and then cut into 1-cm segments, resulting in 170 samples for laboratory analyses.

Sample dating and age model

Thirteen bulk samples were collected at ca. 10-cm intervals from the HL06 sediment core (Fig. 2, Table 1) and dated with an Accelerator Mass Spectrometry (AMS) system (Compact-AMS, NEC Pelletron) at the Paleo Labo Co., Ltd. in Japan. Organic carbon was extracted from each sample and dated following the method described by Nakamura et al. (2000). The $^{14}C/^{12}C$ and $^{13}C/^{12}C$ ratios of each sample, with an oxalic acid standard (SRM-4990C, commonly designated HOxII), were measured with the AMS system. In order to correct the $^{14}C/^{12}C$ ratios for isotopic fractionation, the $\delta^{13}C$ value of each sample was analyzed with the system (Table 1). The ^{14}C dates of all the samples from the HL06 core were determined with a half-life of 5568 yr.

The ^{14}C age of the uppermost 1 cm of the HL06 core could be considered to result from 'hard-water' and other reservoir effects on radiocarbon dating of the lake sediments. To produce an age–depth model for HL06 core, we first subtracted this reservoir age from all the original ^{14}C ages, assuming that it is constant through the core, and then performed calibrations on the reservoir-effect-free ^{14}C dates. The conventional ages were converted to calibrated ages using the OxCal3.1 radiocarbon age calibration program (Bronk Ramsey, 2001) with the IntCal04 calibration data (Reimer et al., 2004). Ages

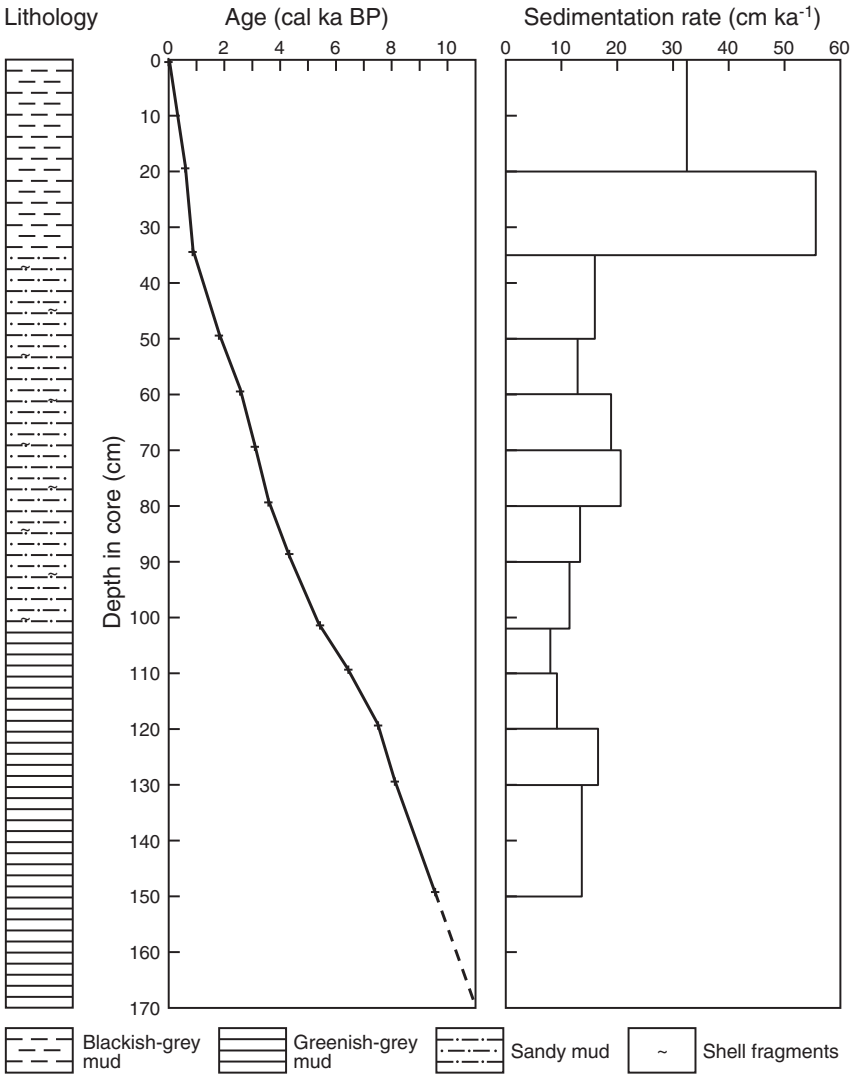

Figure 2. Lithological log and age–depth model of the HL06 sediment core recovered in the central part of Hulun Lake. Crosses represent the mean values of 2σ ranges of calibrated ages of reservoir-effect-free radiocarbon dates. The dashed line was derived from two superjacent calibrated ages by linear extrapolation to yield ages for sampled horizons of the lowermost 20-cm sediment core.

https://doi.org/10.1016/j.yqres.2011.02.008 Published online by Cambridge University Press

Table 1
AMS radiocarbon dates of samples from the HL06 sediment core recovered in the central part of Hulun Lake.

Laboratory number[a]	Depth interval (cm)	Dating material	$\delta^{13}C$ (‰)	AMS ^{14}C age (^{14}C yr BP)	Corrected ^{14}C age[b] (^{14}C yr BP)	Calibrated ^{14}C age (2σ) (cal yr BP)
PLD–7489	1–0	Organic matter	−26.94	685 ± 21	0 ± 30	0–10
PLD–7491	20–19	Organic matter	−25.63	1335 ± 22	650 ± 30	610–550
PLD–7493	35–34	Organic matter	−26.01	1611 ± 22	926 ± 30	930–770
PLD–7494	50–49	Organic matter	−26.40	2543 ± 22	1858 ± 30	1870–1710
PLD–7925	60–59	Organic matter	−26.57	3222 ± 29	2537 ± 36	2650–2480
PLD–7495	70–69	Organic matter	−27.73	3630 ± 27	2945 ± 34	3220–2970
PLD–7926	80–79	Organic matter	−26.72	4034 ± 30	3349 ± 37	3690–3470
PLD–7927	90–89	Organic matter	−25.40	4575 ± 31	3890 ± 37	4430–4230
PLD–7496	102–101	Organic matter	−28.38	5304 ± 27	4619 ± 34	5470–5290
PLD–7928	110–109	Organic matter	−26.34	6338 ± 35	5653 ± 41	6510–6310
PLD–7498	120–119	Organic matter	−30.24	7285 ± 30	6600 ± 37	7570–7430
PLD–7929	130–129	Organic matter	−26.53	8003 ± 38	7318 ± 43	8200–8010
PLD–7499	150–149	Organic matter	−30.99	9268 ± 38	8583 ± 43	9660–9480

[a] PLD: Paleo Labo Dating, laboratory code of Paleo Labo Co., Ltd., Japan.
[b] The reservoir correction factor is 685 yr, ^{14}C age of the uppermost 1 cm of the core sediments.

of sampled horizons of the sediment core were derived by linear interpolation between radiocarbon-dated horizons using the mean values of 2σ ranges of calibrated ages.

Ostracode assemblage analysis

The extraction of fossil ostracode valves follows the method described by Zhai et al. (2010). For each sample of ca. 300 mg of air-dried sediment, 60 ml of 10% H_2O_2–0.1% Na_2CO_3 solution (pH 9–10) was added to disaggregate the sediment for 24 h. The resulting sediment was sieved in water through a 250-mesh sieve (63-μm pore size). The sieve residue was rinsed repeatedly, spread onto a glass plate as thin stripes and dried at 40°C. All the ostracode valves extracted from the samples were identified and counted with an Olympus stereomicroscope at 40× magnification.

The identification of the ostracodes from the samples follows the taxonomy of Meisch (2000) and Hou et al. (2002). *Limnocythere dubiosa* and *L. sancti-patricii* in Xu et al. (1989) and Wang and Ji (1995) were identified as *L. inopinata*, and *Candoniella albicans* as *Pseudocandona albicans*. The *Ilyocypris* species were identified as *I. gibba* and *I. decipiens* under a Scanning Electron Microscopic observation of the "marginal ripplets" on the left valve (Janz, 1994), or noted as *Ilyocypris* spp. when the specimens could not be identified down to the species level.

Numerical analyses

Cluster analysis (CONISS, Grimm, 1987) was used to divide the ostracode-abundance diagram of the HL06 sediment core into ostracode assemblage zones. To ordinate the ostracode data from the sediment core and detect patterns of the local ostracode community evolution, ordination techniques were utilized with the program CANOCO version 4.5 (Ter Braak and Šmilauer, 2002). Eight ostracode groups with abundances >15 valves per gram (valves g^{-1}) in any sample were used for ordination in this study, and a logarithmic transformation was applied to the data. Detrended correspondence analysis showed that the gradient length of the first axis is 2.136, indicating a linear response of the ostracode assemblages to environmental variables (Ter Braak and Šmilauer, 2002). Therefore, principal component analysis (PCA) was chosen for ordination of the ostracode data from the sediment core. The PCA centers both by the samples and by the ostracode species to better represent the real "ecological distance" between the samples and compare differences in the species composition among the samples.

Chemical analyses

Adult valves of *L. inopinata* from the HL06 core sediments were used for chemical analyses. Each sample of 0.3–5 g of air-dried sediment was chemically pretreated following the method described above. The residue was sieved in water through a 120-mesh sieve (125-μm pore size). Adult valves of *L. inopinata* were picked and cleaned in deionized water (18 MΩ) with a fine brush under an Olympus stereomicroscope and dried at 72°C for analyses of Ca, Mg and Sr concentrations and oxygen and carbon isotope compositions.

The concentrations of Ca, Mg and Sr were determined with an Inductively Coupled Plasma Mass Spectrometer (ICP-MS). About 7 valves were dissolved in 2 ml of 3% ultra-pure HNO_3, and the solution was used for determination of element concentrations. Multi-element standards prepared by dilution of GBW(E) mono-element standard solutions (GBW(E)080261 for Ca, GBW(E)080262 for Mg and GBW(E) 080242 for Sr) for ICP-MS were used for calibration after every twenty-sample measurement. The relative error of concentrations of the related elements in the solution is less than 5%. Mg/Ca and Sr/Ca were expressed as atomic ratios.

Oxygen and carbon isotope compositions were determined with a Finnigan MAT 253 mass spectrometer equipped with a Kiel IV carbonate preparation device. About 50 μl of 103% H_3PO_4 was added to 10–15 valves, and the sample solution was kept for reaction in Kiel IV at 72°C for 10 min to generate CO_2 for measurements of $^{18}O/^{16}O$ and $^{13}C/^{12}C$ ratios. $\delta^{18}O$ and $\delta^{13}C$ are expressed in parts per thousand (‰) relative to VPDB (Vienna PeeDee Belemnite). A reference carbonate sample, NBS19, was routinely analyzed after every six-sample measurement. All the $\delta^{18}O$ and $\delta^{13}C$ values were normalized to NBS19, the certified $\delta^{18}O$ and $\delta^{13}C$ values of which are −2.20‰ and 1.95‰. The precision is better than 0.15‰ for $\delta^{18}O$ and 0.10‰ for $\delta^{13}C$.

Results

Lithology and chronology

The sediments of the HL06 core can be divided into three main sedimentary units (Fig. 2). The lower unit at core depths of 170–100 cm is characterized by a greenish-gray color, massive and compact structure and lack of laminations and consists of homogeneous mud. The middle unit at depths of 100–35 cm is characterized by a dark gray to blackish-gray color, massive and compact structure and a lack of laminations and composed of sandy mud. The scattered fragments of ostracode and mollusk shells can be seen in the middle sandy mud. The upper unit at depths of 35–0 cm is blackish gray in color and consists of oozy mud with a high water content.

As shown in Figure 2 and Table 1, the uppermost 1 cm of the HL06 sediment core yields a ^{14}C age of 685 yr. This anomalously old age was considered as the reservoir age of Hulun Lake. The reservoir age of 685 yr was first subtracted from all the original ^{14}C ages, and then calibrations were performed on the reservoir-effect-free ^{14}C dates to produce the age–depth model for the HL06 core (Fig. 2). The

https://doi.org/10.1016/j.yqres.2011.02.008 Published online by Cambridge University Press

age–depth model indicates that the HL06 sediment core covers the last ca. 11,000 yr (Fig. 2). The sedimentation rate ranges from 7.8 to 55.6 cm ka^{-1} with an average of 15.6 cm ka^{-1} during the Holocene (Fig. 2). The sedimentation rates and a sampling interval of 1 cm provide potential temporal resolutions of ca. 128 to 18 yr for the ostracode data of the HL06 sediment core.

Species assemblage and shell chemistry of the ostracodes

HL06 core sediments contain abundant ostracodes. Most samples yielded 300 to 4000 ostracode valves, resulting in a total of 250,041 valves from the 170 samples (Fig. 3). Fourteen species of ostracodes belonging to nine genera were identified. These are *Limnocythere inopinata* (Baird 1843), *Darwinula stevensoni* (Brady and Robertson 1870), *Ilyocypris gibba* (Ramdohr 1808), *Ilyocypris decipiens* Masi 1905, *Candona neglecta* Sars 1887, *Candona* cf. *houae* Huang 1964, *Pseudocandona albicans* (Brady 1864), *Pseudocandona* sp., *Candoniella subellipsoida* Sharapova 1962, *Candoniella mirabilis* Schneider 1963, *Cypridopsis* sp., *Cyclocypris serena* (Koch 1838), *Cyclocypris globosa* (Sars 1863) and *Eucypris* sp. (Fig. 3). *Limnocythere inopinata* is the dominant species and accounts for more than 38% of the total ostracodes.

The ostracode abundance diagram of the HL06 sediment core spanning the last ca. 11,000 yr (Fig. 3) can be divided into three ostracode-assemblage zones with eight subzones based on stratigraphically-constrained cluster analysis (CONISS; Grimm, 1987). PCA ordination of major ostracode taxa and the samples reflects the feature of the ostracode abundance diagram and the pattern of the local ostracode community evolution (Fig. 4). As shown in Figure 4, eight clusters of points corresponding to ostracode assemblage subzones are clearly separated from each other on the biplot of PCA scores along the first two axes that capture 69.0% and 12.5% of the total variance within the ostracode data set.

Data of Mg/Ca and Sr/Ca ratios, $\delta^{18}O$ and $\delta^{13}C$ of adult valves of *L. inopinata* from the HL06 sediment core were plotted against calibrated age in Figure 5. The stages characterizing the pattern of changes in valve chemistry during the Holocene were bracketed by the ostracode-assemblage zones and subzones (Fig. 5).

Zone 3 (ca. 11,100–8300 cal yr BP, 170–132 cm): This zone is characterized by abundant *D. stevensoni* (258–2384 valves g^{-1}) and scarce *Ilyocypris* spp. (<3 valves g^{-1}). *Candona neglecta* (87–440 valves g^{-1}) and *C.* cf. *houae* (13–65 valves g^{-1}) are rich in subzone 3b (11,100–10,400 cal yr BP) and nearly absent in subzone 3a (10,400–8300 cal yr BP) and the subsequent zones. Around 9600–9000 cal yr BP (150–141 cm), the ostracode valves show signs of whitening, pitting and softening.

Mg/Ca, Sr/Ca, $\delta^{18}O$ and $\delta^{13}C$ display an overall decreasing trend in this zone. Anomalously high Mg/Ca ratios occurred 9600–9000 cal yr BP. Sr/Ca decrease to the lowest ratios for the whole Holocene in subzone 3a. $\delta^{18}O$ shows their lowest values of −5.6‰ to −7.0‰ 9900–8950 cal yr BP, accompanied by decreases in $\delta^{13}C$.

Zone 2 (ca. 8300–1900 cal yr BP, 132–51 cm): *Darwinula stevensoni* decreases drastically to below 138 valves g^{-1}, and *Ilyocypris* spp. appear with an average abundance of 24 valves g^{-1}. *Limnocythere inopinata* reaches an average abundance of 6813 valves g^{-1} in this zone and is much more abundant than in zones 3 and 1. In subzone 2d (8300–6200 cal yr BP), *D. stevensoni* continues to decrease, *Ilyocypris* spp. attain to an average abundance of 39 valves g^{-1}, the maximum value for the whole Holocene, and *Ps. albicans* and *C. subellipsoida* first appeared 7000 cal yr BP. In subzone 2c (6200–4300 cal yr BP), *L. inopinata* increases to 6188–7166 valves g^{-1}, and *Ilyocypris* spp. decrease to below 20 valves g^{-1}, accompanied by a gradual disappearance of *D. stevensoni* and frequent occurrences of *Ps. albicans* and *C. subellipsoida*. Subzone 2b (4300–3350 cal yr BP) is marked by the diversity of aquatic fauna including ostracodes (*Ps. albicans*, *Pseudocandona* sp., *C. subellipsoida*, *Cypridopsis* sp., *C. globosa* and *Eucypris* sp.), gastropods and fishes. Later, the diverse aquatic community collapses in subzone 2a (3350–1900 cal yr BP) as *L. inopinata* reaches its peak abundance of 22,689 valves g^{-1} and *Ilyocypris* spp. thrive again with an average abundance of 29 valves g^{-1}.

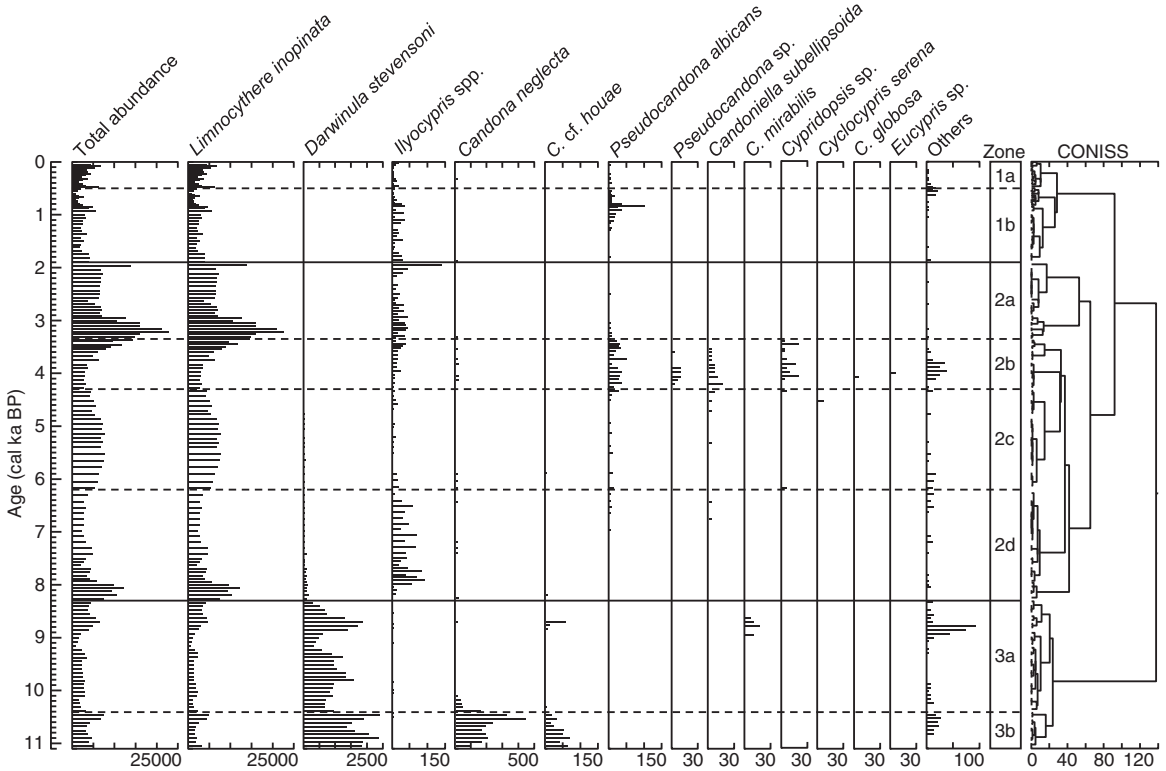

Figure 3. Ostracode-assemblage diagram of the HL06 sediment core spanning the last ca. 11,000 cal yr. Ostracode abundances are expressed in valves per gram (valves g^{-1}) of air-dried samples. The chronology was derived from the age–depth model with the reservoir-age corrected. Cluster analysis (CONISS) is based on the total sum of squares ($\times 10^3$). Horizontal solid and dashed lines bracket the ostracode-assemblage zones and subzones based on CONISS.

https://doi.org/10.1016/j.yqres.2011.02.008 Published online by Cambridge University Press

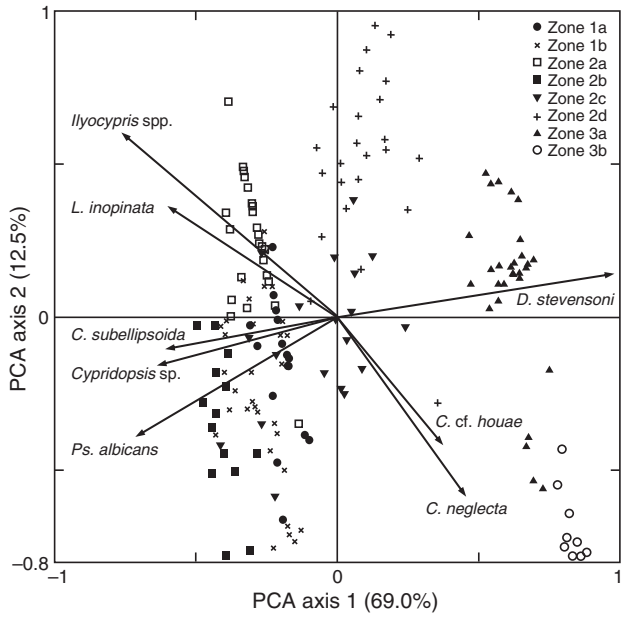

Figure 4. PCA ordination of eight ostracode taxa with abundances >15 valves g^{-1} in any sample and the total ostracode data of the HL06 sediment core recovered in the central part of Hulun Lake. Eigenvalues of the first four axes are 0.690, 0.125, 0.091 and 0.043, respectively. The first and second axes capture 81.4% of the total variance within the data set.

Mg/Ca and Sr/Ca vary with each other in this zone. Both exhibit the Holocene lowest ratios in the early subzone 2d and then increase, while fluctuating, to their peak ratios of 0.024 and 0.0063 at the end of subzone 2c. Subzone 2b is characterized by decreases in Mg/Ca and Sr/Ca to around 0.011 and 0.0035. Mg/Ca and Sr/Ca increase to their peak ratios ca. 3000 cal yr BP and then decrease to the Holocene lowest ratios of 0.011 and 0.0032 at the end of subzone 2a. $\delta^{18}O$ fluctuate within the range of −6.3‰ to −4.4‰ in zone 2. The average $\delta^{18}O$ value was −4.3‰ at the early half of subzone 2d and increased to −3.4‰ at the late half. $\delta^{18}O$ displays a decreasing trend in subzones 2c and 2a and an increasing trend in subzone 2b. $\delta^{13}C$ values were remarkably low in the early subzone 2d and subzone 2b, averaging −5.0‰ and −5.1‰. The $\delta^{13}C$ shows low-amplitude variations around −3.0‰ in the late subzone 2d and subzones 2c and 2a.

Zone 1 (ca. 1900–0 cal yr BP, 51–0 cm): *Limnocythere inopinata* decreased dramatically to an average abundance of 2683 valves g^{-1}. At ca. 1100–800 cal yr BP in subzone 1b (1900–500 cal yr BP), *Ps. albicans* that disappears in subzone 2a returns again and reaches its peak abundance of 101 valves g^{-1}. In subzone 1a (500–0 cal yr BP), *L. inopinata* increased from 1469 to 6831 valves g^{-1}, and both *Ilyocypris* spp. and *Ps. albicans* largely decreased.

In zone 1, Mg/Ca, Sr/Ca and $\delta^{13}C$ display low values with the averages of 0.015, 0.003 and −4.9‰, respectively, whereas the $\delta^{18}O$ shows high values with an average of −4.4‰. At the interval of 1100–800 cal yr BP, Mg/Ca and Sr/Ca ratios and $\delta^{18}O$ and $\delta^{13}C$ values were relatively higher, averaging 0.017, 0.0034, −4.2‰ and −4.8‰, respectively. All these indicators exhibit a general trend of decreases in their values during the past 500 yr.

Discussion

Ecological implications of ostracode taxa

Most of the non-marine ostracodes live at the bottom of water bodies or in the top centimeters of the sediments, and their occurrence is thus related to the depth, salinity and/or temperature of the host water (Meisch, 2000). *Limnocythere inopinata* was mainly found from shallow waters with water depths <4 m in Lake Constance (Löffler, 1969), <6 m in Lake Mondsee (Danielopol et al., 1993) and <9 m in Lake Dali (Zhai et al., 2010). *Limnocythere inopinata* has a bias towards brackish waters with conductivities >2000 μs cm^{-1} (Mischke et al., 2007) and can tolerate a salinity up to 100‰ (Forester et al., 2005). As a polythermophilic species, *L. inopinata* mainly occurs and reproduces in summer (Meisch, 2000).

Darwinula stevensoni occurs at water depths <12 m and shows its maximum abundance at water depths of 6–7 m in some lakes (McGregor, 1969; Rieradevall and Roca, 1995). Dense populations of *D. stevensoni* were reported from fresh and slightly brackish lakes such as Lake Gull in America (McGregor, 1969), Lake Pääjärvi in Finland (Ranta, 1979) and Pond Grand Mellaerts in Belgium (Van

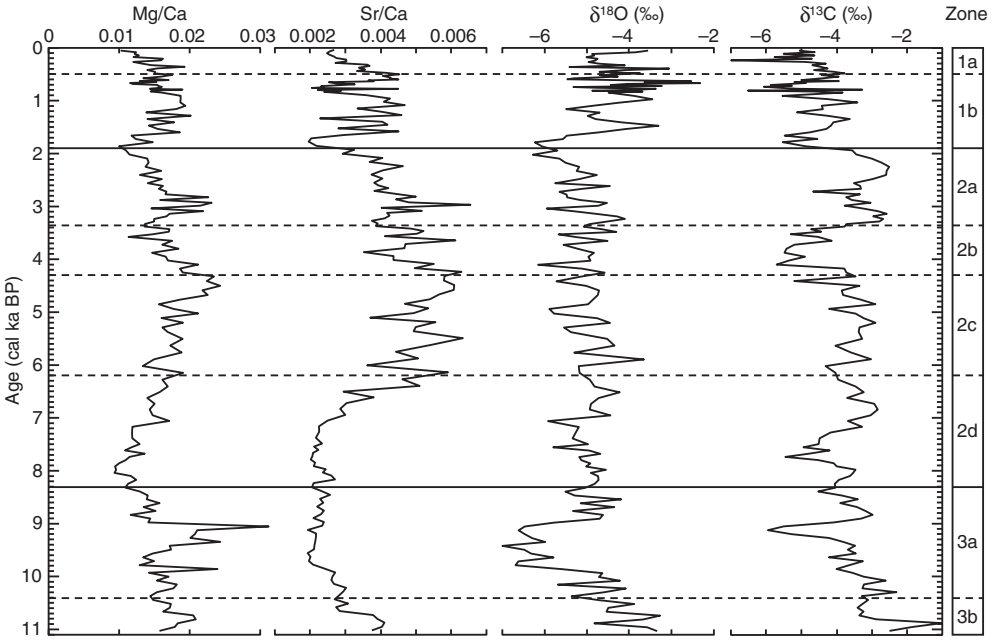

Figure 5. Shell chemistry (Mg/Ca, Sr/Ca, $\delta^{18}O$ and $\delta^{13}C$) of the dominant ostracode *L. inopinata* from the HL06 sediment core spanning the last ca. 11,000 cal yr. The chronology was derived from the age–depth model with the reservoir-age corrected. Horizontal solid and dashed lines indicate the ostracode-assemblage zones and subzones based on CONISS.

https://doi.org/10.1016/j.yqres.2011.02.008 Published online by Cambridge University Press

Doninck et al., 2003), although some specimens were found in waters with a salinity up to 15‰ (Hiller, 1972). It was suggested that *D. stevensoni* occurs frequently in waters with salinities <1‰ and becomes rare when the salinity is higher (Forester et al., 2005; Mezquita et al., 2005). The preference of *D. stevensoni* for water temperature remains unclear. In Lake Banyoles in Spain, *D. stevensoni* increases to its maximum abundance in October–February when the temperature of bottom waters falls below 15°C (Rieradevall and Roca, 1995). In Pond Grand Mellaerts, however, the maximum abundance of *D. stevensoni* occurs in April–August when the water temperature rises to around 20°C (Van Doninck et al., 2003).

Ilyocypris gibba usually lives in small, shallow water bodies and also appears in large, deep lakes (Wilkinson et al., 2005). *Ilyocypris gibba* can tolerate small changes in salinity within the oligohaline range (Wilkinson et al., 2005) and prefers warm temperatures although it occurs in waters of 7.5–42°C (Külköylüoğlu, 2004). *Ilyocypris decipiens* was reported from lakes, ponds and rivers with water salinities <2.2‰ (Hiller, 1972). Similarly to *I. gibba*, *I. decipiens* was described as a polythermophilic species (Meisch, 2000). Both *I. gibba* and *I. decipiens* appear in summer (Meisch, 2000).

Candona neglecta dwells in various water bodies including springs, ponds and lakes' littoral and profundal zones with a salinity range of 0.5–16‰. It prefers cold waters and can only tolerate temporary increases in temperature above 20°C (Meisch, 2000). *Candona neglecta* can be found all through the year when it is cool in summer (Hiller, 1972).

Pseudocandona albicans lives in small water bodies and the littoral zone of lakes with a maximum salinity of 5.5‰ (Hiller, 1972). Adult and juvenile *Ps. albicans* live together throughout the year (Nüchterlein, 1969), implying a wide tolerance of *Ps. albicans* to water temperature. *Pseudocandona* sp. would correspond to one of the four species, *Ps. marchica*, *Ps. rostrata*, *Ps. sarsi* and *Ps. hartwigi*. Similarly to *Ps. albicans*, these ostracodes all occur in small water bodies or the littoral zone of lakes (Meisch, 2000).

Members of the genus *Cypridopsis* usually reside in shallow waters because of their ability to resist wave scourings (Meisch, 2000). *Cypridopsis* sp. found from Hulun Lake in this study would assume the ecological features similar to its relatives.

The ecological preferences of *C.* cf. *houae* and *C. subellipsoida* remain unclear. As shown on the PCA biplot (Fig. 4), however, *C.* cf. *houae* is close to cold-adapted *C. neglecta*, and *C. subellipsoida* close to the littoral species *Ps. albicans* and *Cypridopsis* sp. Such an ordination of the ostracode taxa may denote that *C.* cf. *houae* prefers to cold waters and *C. subellipsoida* to shallow waters.

Water chemical implications of Mg/Ca, Sr/Ca, $\delta^{18}O$ and $\delta^{13}C$ of the ostracode valves

Ca, Mg and Sr in calcite shells of ostracodes are derived from the host water, and the Mg/Ca and Sr/Ca ratios of ostracode shells are positively related to those of the host water (Chivas et al., 1986; Xia et al., 1997b). The waters of lakes in arid/semi-arid regions are usually saturated with respect to $CaCO_3$, resulting in the precipitation of carbonates within a lake and the removal of calcium from the lake water. Consequently when the salinity of lake water increases due to evaporative enrichment, Ca^{2+} will either increase in lake water at a lower rate than Mg^{2+} and Sr^{2+} given the alkalinity/Ca^{2+} ratio of lake water <1, or decrease in lake water given the alkalinity/Ca^{2+} ratio of lake water >1 (Ito and Forester, 2009). In both cases, especially in the latter case, the Mg/Ca and Sr/Ca ratios of lake waters increase with the increase in water salinity (Ito and Forester, 2009). Therefore increases in Mg/Ca and Sr/Ca ratios of ostracode shells indicate increases in those of lake water and thus in water salinity. On the other hand, the Mg/Ca ratio of both lake waters and ostracode shells is positively related to water temperature and such a correlation decreases in the lake water of high Mg/Ca ratios (Chivas et al., 1986; Gouramanis and De Deckker, 2010). In inland lakes, the water temperature has a much less significant effect on the Mg/Ca ratio of calcite shells of ostracodes than the water salinity, and the temperature effect on the Sr/Ca ratio is almost negligible (Chivas et al., 1986; De Deckker et al., 1999). Nevertheless in lakes with high Mg/Ca ratios (>20) or high salinities (>20 g l^{-1}), the relations between trace element ratios of lake waters/ostracode shells and the water salinity or temperature could be modified by other factors such as the precipitation of aragonite (Xia et al., 1997b), formation of ion complexes (Ito and Forester, 2009) and the concentration of HCO_3^- (Gouramanis and De Deckker, 2010). Hulun Lake in the present study has a salinity of 2.45 g l^{-1}, a Mg/Ca ratio of 8.75 and an alkalinity/Ca^{2+} ratio of 24. The precipitation of carbonates within the lake occurs in the form of calcite during the whole Holocene (unpublished data of carbonate minerals in a parallel sediment core HL08). These data suggest that the Mg/Ca and Sr/Ca ratios of the ostracode shells from Hulun Lake are positively related to the water salinity with the Mg/Ca ratio related to the water temperature as well.

The $\delta^{18}O$ of ostracode shells depends on both the $\delta^{18}O$ and the temperature of the host water. An increase of 1‰ in ostracode $\delta^{18}O$ could be caused either by an increase of 1‰ in water $\delta^{18}O$ or a decrease of 4–5°C in water temperature or a combination of both (Xia et al., 1997a). The $\delta^{18}O$ of lake water is closely related to the precipitation/evaporation (P/E) ratio in arid/semi-arid regions (Lister et al., 1991; Xia et al., 1997b; Holmes et al., 2007), although it can be altered by various factors such as source water, temperature and humidity in the lake area (Ricketts et al., 2001). When the P/E ratio decreases, the $\delta^{18}O$ of lake water increases because more $H_2^{16}O$ is evaporated so that the lake water becomes enriched in ^{18}O. It is noticeable that changes in source water could blur the effect of P/E ratio on the $\delta^{18}O$ of lake water especially in large lakes that usually collect various sources of water including rainfalls, snow/ice melt and groundwater from large catchments (Ricketts et al., 2001).

The $\delta^{13}C$ of ostracode shells is mainly controlled by that of dissolved inorganic carbon (DIC) in the ambient water (Von Grafenstein et al., 1999). In oligotrophic lakes, the ^{13}C exchange between DIC and atmospheric CO_2 is considered as the most important factor that affects the $\delta^{13}C$ of DIC although the primary productivity, degradation of organic matter, calcite precipitation in lakes and the $\delta^{13}C$ of input waters have influence on the DIC $\delta^{13}C$ (Talbot, 1990; Fontes et al., 1996). The $\delta^{13}C$ of atmospheric CO_2 is −7‰, and the fractionation factor between DIC and CO_2 is 8–10‰, yielding a $\delta^{13}C$ of 1–3‰ for DIC in equilibrium with CO_2 (Ricketts et al., 2001). The $\delta^{13}C$ values of DIC are usually below the equilibrium value, but become larger when the ^{13}C exchange is intensified (Ricketts et al., 2001). The lowering of lake level and alkalifying of lake water would facilitate the ^{13}C exchange between DIC in lake-bottom water and atmospheric CO_2, leading to an increase in the $\delta^{13}C$ of DIC (Fontes et al., 1996; Xia et al., 1997b).

Holocene hydrological and climatic changes

The species assemblage and shell chemistry of ostracodes from the HL06 sediment core reveal a detailed history of changes in the lake level and water salinity and temperature of Hulun Lake during the Holocene (Figs. 3, 5 and 6). Historical documents and modern observations indicate that Hulun Lake expanded and lake water became fresh during high rainfall years (Xu et al., 1989). These data imply that past changes in the lake level and water salinity of Hulun Lake are closely related to climatic changes in the lake area. From 11,100 to 10,400 cal yr BP, *D. stevensoni* was abundant, *L. inopinata* was less abundant, littoral ostracode taxa were absent, and Mg/Ca and Sr/Ca ratios were relatively lower, indicating that the lake water was fresh or slightly brackish and its level was high. The warm-adapted *Ilyocypris* spp. (*I. gibba* and *I. decipiens*) were scarce, whereas the cold-adapted *C. neglecta* and *C.* cf. *houae* throve, suggesting cool waters in the lake. The heavy $\delta^{18}O$ of the

https://doi.org/10.1016/j.yqres.2011.02.008 Published online by Cambridge University Press

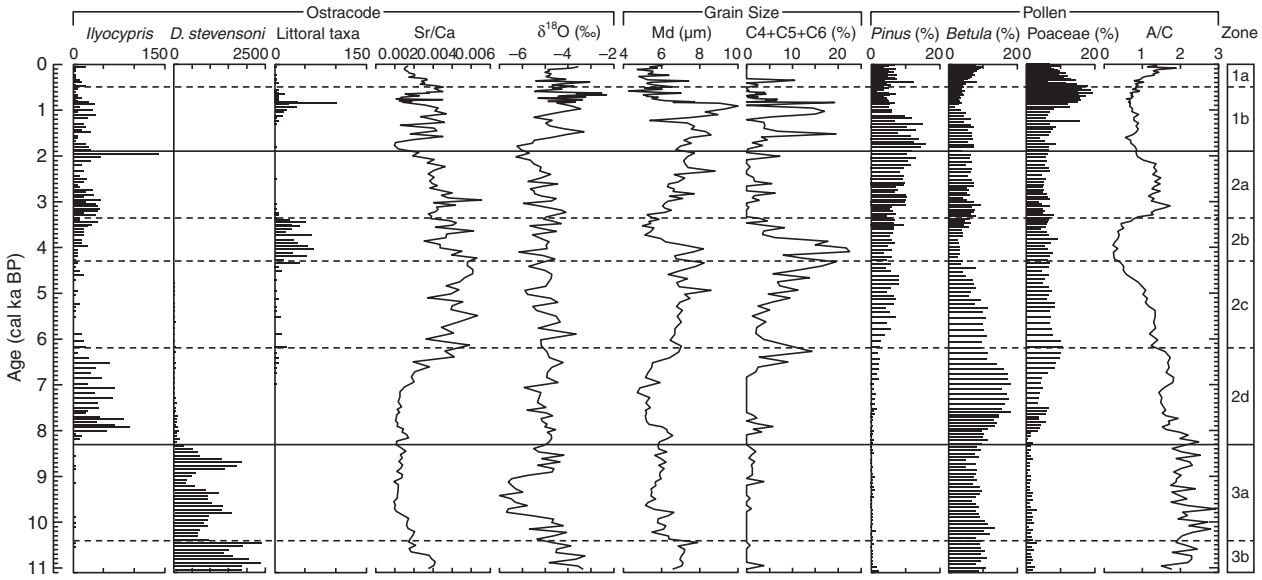

Figure 6. Abundances of *Ilyocypris*, *D. stevensoni* and littoral taxa and Sr/Ca and $\delta^{18}O$ of *L. inopinata* from the HL06 sediment core spanning the last ca. 11,000 cal yr, compared with the median grain size (Md) and nearshore grain-size components (C4 + C5 + C6) (Xiao et al., 2009) and percentages of *Pinus*, *Betula* and Poaceae and the ratio of *Artemisia* to Chenopodiaceae (A/C) (Wen et al., 2010a) of the same core. Horizontal solid and dashed lines indicate the ostracode-assemblage zones and subzones based on CONISS.

ostracodes might result from the heavy $\delta^{18}O$ and the low temperature of the lake water.

From 10,400 to 8300 cal yr BP, *D. stevensoni* was still abundant, *L. inopinata* declined, littoral taxa were absent, and Sr/Ca, $\delta^{18}O$ and $\delta^{13}C$ all decreased significantly, indicating that the lake continued to assume high stands and the water salinity decreased. *Candona neglecta* and *C.* cf. *houae* became largely reduced and *Ilyocypris* spp. occasionally appeared, implying a certain rise in the water temperature. The drastic decrease in the $\delta^{18}O$ from 9900 to 8950 cal yr BP might reflect the input of low-$\delta^{18}O$ waters to the lake in terms of relatively little decreases in the Sr/Ca and $\delta^{13}C$. The dilution of the lake water during this interval would be responsible for the partial dissolution of ostracode shells from 9600 to 9000 cal yr BP, which significantly modified the Mg/Ca ratios.

Proxy records of the ostracodes from the HL06 sediment core indicate that Hulun Lake assumed high stands and the water had low salinities and cool temperatures during the early Holocene before 8300 cal yr BP. Sedimentological studies of the same core (Xiao et al., 2009) show that the proportion of the nearshore grain-size components in the sediments was low and the median grain size was relatively fine during the early Holocene (Fig. 6). Palynological data from the same core (Wen et al., 2010a) indicate that the lake basin was dominated by dry steppe with the less coverage of grasses during the early Holocene (Fig. 6). Based on these data, we infer that the cool and fresh waters entering the lake during the early Holocene might result from the input of the snow/ice melt from the surrounding mountains. The Urshen and Hailar Rivers (Fig. 1) rise in the Greater Hinggan Mountains where the elevation reaches 1200–1300 m and the annual precipitation exceeds 500 mm. Hydrological observations indicate that the discharge of both rivers is as large during spring floods as during summer floods because of melt runoff from the snow/ice packs covering the mountains (Xu et al., 1989). During the early Holocene with the increase in summer solar radiation in the Northern Hemisphere (Kutzbach and Street-Perrott, 1985), the snow and ice accumulated on the mountains would melt gradually and supply the lake with cool and fresh waters that kept the lake at high stands.

From 8300 to 6200 cal yr BP, *D. stevensoni* declined to almost inexistent abundances and *Ilyocypris* spp. flourished, implying an obvious increase in water temperature. During the period of 8300–7100 cal yr BP, littoral ostracodes were absent, and Mg/Ca, Sr/Ca, $\delta^{18}O$ and $\delta^{13}C$ were low, denoting a status of high lake levels and fresh waters similar to the early Holocene. Afterwards, littoral ostracodes such as *Ps. albicans* and *C. subellipsoida* first appeared, and trace element ratios and stable isotope compositions increased simultaneously, denoting a slow increase in water salinity and a slight drop in lake level. Both the proportion of the nearshore components in the sediments and the median grain size remain low values during this episode, indicating the high stands of the lake similar to the early Holocene (Xiao et al., 2009; Fig. 6). Grasses and birch forests expanded in the lake basin from 8000 to 6400 cal yr BP, suggesting warm and wet climatic conditions in the lake area during this period (Wen et al., 2010a; Fig. 6). The shift from cool and fresh to warm and fresh lake waters occurring 8300 cal yr ago implies that the precipitation in the lake region replaced the snow/ice melt from the surrounding mountains and started to feed the lake at that time, and maintained the high lake levels.

From 6200 to 4300 cal yr BP, *L. inopinata* increased significantly, *D. stevensoni* disappeared gradually, littoral ostracodes occurred frequently, and Mg/Ca, Sr/Ca and $\delta^{13}C$ increased continuously, suggesting that the lake continued to contract and the water became brackish. *Ilyocypris* spp. declined drastically, indicating the onset of cooling of the lake water 6200 cal yr ago. The $\delta^{18}O$ displayed a trend of gradual decreases albeit the increase in water salinity and the decrease in water temperature, presumably denoting the significant supply of the Hailar River through the Dalanolom River for the lake. During this episode, the nearshore components in the sediments and the median grain size continued to increase (Xiao et al., 2009; Fig. 6). Pine patches expanded and birch forests contracted in the lake region, and the *Artemisia*/Chenopodiaceae (A/C) ratio continued to decrease although the grasses remained largely unchanged (Wen et al., 2010a; Fig. 6). All these data lend support for the ostracode-based inference about the decline in lake level, increase in water salinity and the decrease in water temperature from 6200 to 4300 cal yr BP that could be related to dry and cool climatic conditions in the lake area during this period.

The interval between 4300 and 3350 cal yr BP was marked by the lowest lake levels of the entire Holocene due to the highest abundance of littoral ostracodes and the diversity of aquatic fauna. *Candona neglecta* occurred frequently, and *Ilyocypris* spp. were less abundant, denoting relatively cooler lake waters. The obvious decreases in the abundance of *L. inopinata* and in the value of Mg/Ca, Sr/Ca and $\delta^{13}C$ should be indicative of decreased water salinity. Such a decrease in water salinity, however, seemingly contradicts the drop in lake level. HL06 sediment core is located downstream of the Dalanolom and Urshen Rivers (Fig. 1), and the core site could be close to the river mouths and receives the supply of river waters directly when the lake

https://doi.org/10.1016/j.yqres.2011.02.008 Published online by Cambridge University Press

shrank substantially. The decreases in Mg/Ca, Sr/Ca and $\delta^{13}C$ could result, on one hand, from the close proximity of the core site to the river mouths due to the drastic shrinkage of the lake, or on the other hand, from the reduced evaporation in the lake area under cooler climatic conditions. The nearshore components in the sediments attained their highest proportions of the entire Holocene from 4500 to 3800 cal yr BP (Xiao et al., 2009; Fig. 6). Birch forests contracted largely in the lake basin, and arid-tolerant Chenopodiaceae plants expanded, leading to the Holocene lowest A/C ratios from 4400 to 3350 cal yr BP (Wen et al., 2010a; Fig. 6). These data provide support for the ostracode-based inference about the largest lowering of the lake level during the interval between 4300 and 3350 cal yr BP that would have resulted from extremely dry climatic conditions in the lake region.

From 3350 to 1900 cal yr BP, the lake level rose significantly as suggested by the dramatic decrease of littoral ostracodes. *Limnocythere inopinata* throve first and then declined, accompanied by increases and subsequent decreases in Mg/Ca and Sr/Ca ratios, presumably indicating a continuous decrease in water salinity after a brief increase. *Ilyocypris* spp. became abundant, and *C. neglecta* almost disappeared, suggesting an increase in water temperature. During this episode, the proportion of the nearshore components in the sediments decreased substantially although the median grain size became coarse due to increases in the relative percentage of the silt-fraction particles, indicating an expansion of the lake (Xiao et al., 2009; Fig. 6). Birch forests expanded in the lake area, and the A/C ratio increased significantly, suggesting increases in the regional humidity and temperature (Wen et al., 2010a; Fig. 6).

From 1900 to 500 cal yr BP, both *L. inopinata* and *Ilyocypris* spp. largely reduced, and Mg/Ca and Sr/Ca ratios and $\delta^{13}C$ values were low, implying a slight decrease in water temperature and salinity. The $\delta^{18}O$ displayed a trend of gradual increases, probably denoting the input of high-$\delta^{18}O$ waters into the lake. During the episode of 1100–800 cal yr BP, *Ps. albicans*, *Ilyocypris* spp. and *L. inopinata* all increased, and the chemical indicators showed peak values, suggesting a brief drop in lake level and a rise in water temperature and salinity. Both the nearshore components in the sediments and the median grain size attained their maximum values from 1150 to 900 cal yr BP, indicating an obvious shrinkage of the lake (Xiao et al., 2009; Fig. 6). Birch forests contracted gradually in the lake region, and the A/C ratio decreased substantially after 2050 cal yr BP, suggesting decreases in temperature and humidity (Wen et al., 2010a; Fig. 6).

During the last 500 yr, *Ps. albicans* decreased, indicating a rise in lake level. Chemical indicators all showed a general trend of decreases in their values, suggesting the freshening of the lake water. The gradual flourishing of *L. inopinata* could result from the stability of the lake bottom water due to the persistent expansion of the lake or the warming of lake waters. We infer that the humidity and temperature have gradually increased in the lake region during the recent 500 yr. This inference is supported both by the sedimentological data of decreased nearshore-component proportions in the sediments and fining median grain sizes (Xiao et al., 2009; Fig. 6) and by the palynological data of expanded birch forests and increased A/C ratios (Wen et al., 2010a; Fig. 6).

Possible mechanism for Holocene East Asian monsoon variation

Hulun Lake is located in the northern marginal zone of the East Asian summer monsoon. Modern observations indicate that more than 80% of the annual precipitation falls in summer in the lake area when the monsoon rainfall belt migrates to its northern limit (Chinese Academy of Sciences, 1984; Zhang and Lin, 1985). These data imply that past changes in precipitation in the Hulun Lake region are closely related to variations in the strength of the East Asian summer monsoon. An increase in the regional precipitation would be indicative of the intensification of the summer monsoon.

It was suggested that East Asian monsoon variations are controlled by changes in summer solar radiation in the Northern Hemisphere on glacial–interglacial timescales (An, 2000). The summer solar radiation in the Northern Hemisphere began to increase 12,000 yr ago and reached a maximum 11,000–10,000 yr ago (Kutzbach and Street-Perrott, 1985). However, our ostracode record together with the paleo-precipitation reconstruction based on the pollen profile (Wen et al., 2010b) indicates

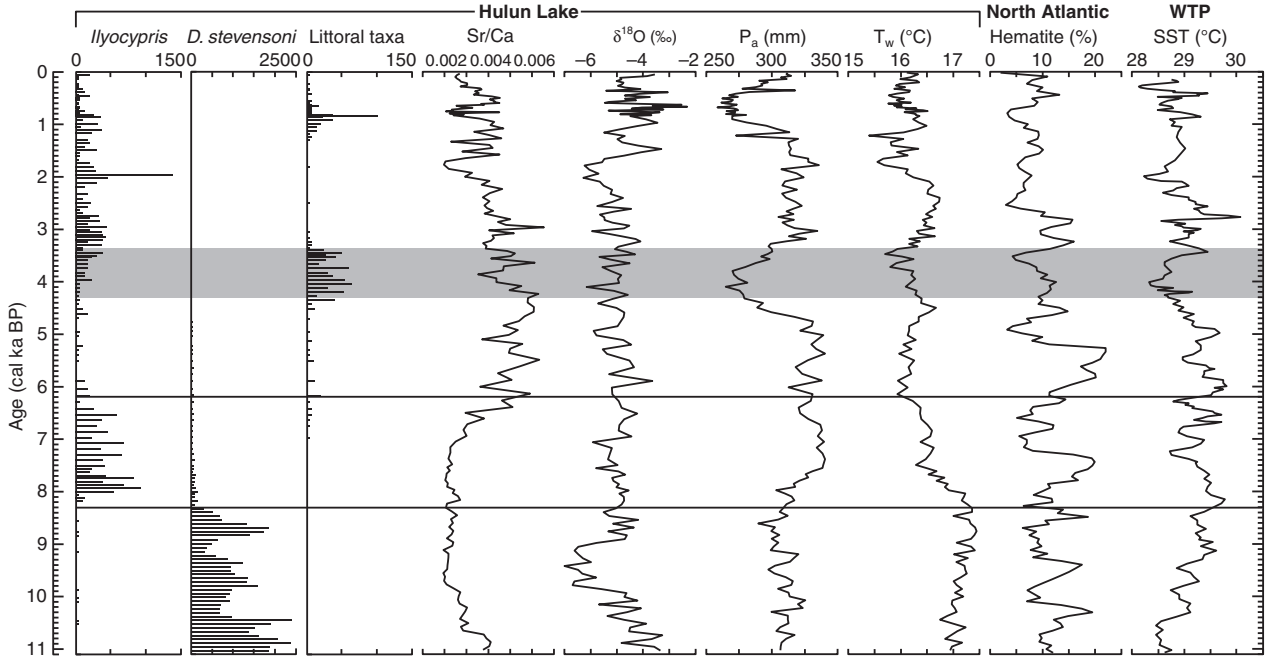

Figure 7. Correlation of *Ilyocypris*, *D. stevensoni* and littoral taxa abundances and Sr/Ca and $\delta^{18}O$ of *L. inopinata* from the HL06 sediment core with the mean annual precipitation (P_a) and mean July temperature (T_w) reconstructed on the pollen profile of the same core (Wen et al., 2010b), hematite-stained grain concentration (Hematite) in VM29-191 core from the North Atlantic (Bond et al., 2001) and sea-surface temperature (SST) reconstructed on the Mg/Ca ratio of *Globigerinoides rubber* from MD98-2176 core in the western tropical Pacific (WTP) (Stott et al., 2004). Horizontal lines indicate significant shifts in the intensity of the East Asian summer monsoon during the Holocene. The horizontal shaded bar marks the interval of a drastic decline in the summer monsoon precipitation during the middle Holocene.

https://doi.org/10.1016/j.yqres.2011.02.008 Published online by Cambridge University Press

that the East Asian summer monsoon did not reach its maximum intensity and the monsoon rainfall belt did not penetrate into its modern northern limit until 8300 cal yr ago (Fig. 7), showing a time lag of ca. 3000 yr behind the maximum summer solar radiation in the Northern Hemisphere. Changes in the concentration of hematite-stained grains in VM29-191 sediment core from the North Atlantic document frequent ice drift events before 8000 cal yr BP (Bond et al., 2001; Fig. 7), indicating the existence of substantial ice masses in the northern high latitudes during the early Holocene (COHMAP Members, 1988). On the other hand, the Mg/Ca ratios of planktonic *Globigerinoides ruber* in MD98-2176 sediment core from the western tropical Pacific show that the sea surface temperature increased gradually during the early Holocene and reached the warmest values around 8000 cal yr BP (Stott et al., 2004; Fig. 7). The time lag between the East Asian summer monsoon intensification and the maximum summer solar radiation in the Northern Hemisphere might thus result from a stagnant northward retreat of the polar front in the North Pacific Ocean due to the existence of remnant ice sheets in the Northern Hemisphere, which would hamper the northward penetration of the summer monsoonal front, thereby suppressing monsoon precipitation over northern China. The intensification of the East Asian summer monsoon during the Holocene would be related to the final retreat of large-scale Northern Hemisphere ice sheets 8000 yr ago (COHMAP Members, 1988).

Summer solar radiation in the Northern Hemisphere largely decreased after 6000 cal yr BP (Kutzbach and Street-Perrott, 1985). Our ostracode record and the pollen-based quantitative paleoclimatic reconstruction (Wen et al., 2010b) indicate that the summer monsoon started to weaken and the climate became cool 6200 cal yr ago (Fig. 7), displaying a close link with orbitally induced variations in insolation. This may imply that the weakening of the East Asian summer monsoon during the late middle-Holocene was controlled by changes in summer solar radiation in the Northern Hemisphere.

On millennial scales, on the other hand, East Asian monsoon variations might be associated with the ocean–atmosphere interactions occurring in the tropical Pacific because the moisture/rainfall brought by the summer monsoon onto the land derives from low latitudes of the western Pacific (Chinese Academy of Sciences, 1984; Zhang and Lin, 1985). During the period between 4300 and 3350 cal yr BP, the dramatic fall in the lake level and the extreme decrease in the regional precipitation (Wen et al., 2010b) reveal a large decline of the East Asian summer monsoon (Fig. 7). The surface waters in the western tropical Pacific became cool substantially around 4000 cal yr BP as indicated by the Mg/Ca ratios of planktonic *Globigerinoides ruber* (Stott et al., 2004; Fig. 7). The large weakening of the East Asian summer monsoon coincides, within age uncertainties, with remarkable decreases in the temperature of western tropical Pacific surface waters (Fig. 7), implying a physical link between the summer monsoon variability on millennial scales and the ocean–atmosphere interacting processes in the tropical Pacific. Decreased sea surface temperatures in the low-latitude western Pacific could reduce the formation of water vapor over the source area of the East Asian summer monsoon, thereby decreasing the moisture available for transport via the monsoon circulation from the western tropical Pacific onto the Asian inland and leading to a weakened summer monsoon.

Conclusions

Species assemblage and shell chemistry of the ostracodes from a sediment core at Hulun Lake uncover a detailed Holocene history of changes in the lake's hydrology and the regional climate. During the early Holocene before 8300 cal yr BP, abundant *Darwinula stevensoni*, scarce *Ilyocypris* spp., absent littoral ostracodes and low Mg/Ca, Sr/Ca and $\delta^{18}O$ values indicate that the lake assumed high stands with cool and fresh waters that might result from the input of the snow/ice melt from the surrounding mountains. *Darwinula stevensoni* declined dramatically, *Ilyocypris* spp. appeared largely, littoral ostracodes were still rare, and chemical indicators remained low values during the period from 8300 to 6200 cal yr BP, suggesting that the lake succeeded the status of high levels but the water became warm. The shift from cool and fresh to warm and fresh lake waters occurring 8300 cal yr ago implies that the East Asian summer monsoon was intensified and the monsoon rainfalls in the lake region replaced the snow/ice melt to feed the lake at that time. The lake level dropped to the lowest of the entire Holocene from 4300 to 3350 cal yr BP as documented by the most abundant littoral ostracodes and the diversity of aquatic fauna in the lake, denoting that the East Asian summer monsoon was largely weakened during this interval. The occurrence and distribution of ostracodes in lakes are affected by various factors related to the physical and chemical processes occurring within lakes. Future studies should be focused on the investigation of ecology of the living ostracodes in different lakes from different regions in order to improve our understanding of the ecological tolerance of ostracodes with respect to water depth, salinity and temperature.

Acknowledgments

We thank two anonymous reviewers for valuable comments and suggestions that helped improve the early version of the manuscript. Special thanks are extended to Alan Gillespie, Xiaoping Yang and both reviewers for their careful revisions of the manuscript. This study was financially supported by the Ministry of Science and Technology of China (grant 2010CB833400) and the National Natural Science Foundation of China (grant NSFC 40972120).

References

An, Z.S., 2000. The history and variability of the East Asian paleomonsoon climate. Quaternary Science Reviews 19, 171–187.
Bond, G., Kromer, B., Beer, J., Muscheler, R., Evans, M.N., Showers, W., Hoffmann, S., Lotti-Bond, R., Hajdas, I., Bonani, G., 2001. Persistent solar influence on North Atlantic climate during the Holocene. Science 294, 2130–2136.
Bronk Ramsey, C., 2001. Development of the radiocarbon calibration program. Radiocarbon 43, 355–363.
Chinese Academy of Sciences (Compilatory Commission of Physical Geography of China), 1984. Physical Geography of China: Climate. Science Press, Beijing, pp. 1–30 (in Chinese).
Chivas, A.R., De Deckker, P., Shelley, J.M.G., 1986. Magnesium content of non-marine ostracod shells: a new palaeosalinometer and palaeothermometer. Palaeogeography, Palaeoclimatology, Palaeoecology 54, 43–61.
COHMAP Members, 1988. Climatic changes of the last 18, 000 years: observations and model simulations. Science 241, 1043–1052.
Compilatory Commission of Vegetation of China, 1980. Vegetation of China. Science Press, Beijing, pp. 932–955 (in Chinese).
Danielopol, D.L., Handl, M., Yin, Y., 1993. Benthic ostracods in the pre-alpine deep lake Mondsee: notes on the origin and distribution. In: McKenzie, K.G., Jones, P.J. (Eds.), Ostracoda in the Earth and Life Sciences. Proceedings of the 11th International Symposium on Ostracoda, Rotterdam, pp. 465–480.
De Deckker, P., Chivas, A.R., Shelley, J.M.G., 1999. Uptake of Mg and Sr in the euryhaline ostracod *Cyprideis* determined from *in vitro* experiments. Palaeogeography, Palaeoclimatology, Palaeoecology 148, 105–116.
Delorme, L.D., 1969. Ostracodes as Quaternary paleoecological indicators. Canadian Journal of Earth Sciences 6, 1471–1476.
Fontes, J.C., Gasse, F., Gibert, E., 1996. Holocene environmental changes in Lake Bangong basin (Western Tibet), part 1, chronology and stable isotopes of carbonates of a Holocene lacustrine core. Palaeogeography, Palaeoclimatology, Palaeoecology 120, 25–47.
Forester, R.M., Smith, A.J., Palmer, D.F., Curry, B.B., 2005. North American Non-Marine Ostracode Database "NANODe" Version 1. Kent State University, Kent. Available at http://www.kent.edu/NANODe.
Grimm, E.C., 1987. CONISS: a FORTRAN 77 program for stratigraphically constrained cluster analysis by the method of incremental sum of squares. Computers and Geosciences 13, 13–35.
Gouramanis, C., De Deckker, P., 2010. Alkalinity control on the partition coefficients in lacustrine ostracodes from Australia. Geology 38, 359–362.
Hiller, D., 1972. Untersuchungen zur Biologie und zur Ökologie limnischer Ostracoden aus der Umgebung von Hamburg. Archiv für Hydrobiologie, Supplement-Band 40, 400–497.
Holmes, J.A., 2001. Ostracoda. In: Smol, J.P., Birks, H.J.B., Last, W.M. (Eds.), Tracking Environmental Change Using Lake Sediments. : Zoological Indicators, 4. Kluwer Academic Publishers, Dordrecht, pp. 125–151.

Holmes, J.A., Zhang, J.W., Chen, F.H., Qiang, M.R., 2007. Paleoclimatic implications of an 850-year oxygen-isotope record from the northern Tibetan Plateau. Geophysical Research Letters 34, L23403. doi:10.1029/2007GL032228.
Hou, Y.T., Gou, Y.X., Chen, D.Q., 2002. Fossil Ostracoda of China (Vol. 1). Science Press, Beijing. 1090 pp. (in Chinese).
Ito, E., Forester, R.M., 2009. Changes in continental ostracode shell chemistry: uncertainty of cause. Hydrobiologia 620, 1–15.
Janz, V.H., 1994. Zur Bedeutung des Schalenmerkmals 'Marginalrippen' der Gattung *Ilyocypris* (Ostracoda, Crustacea). Stuttgarter Beiträge zur Naturkunde, Serie B 206, 1–19.
Kutzbach, J.E., Street-Perrott, F.A., 1985. Milankovitch forcing of fluctuations in the level of tropical lakes from 18 to 0 kyr BP. Nature 317, 130–134.
Külköylüoğlu, O., 2004. On the usage of ostracods (Crustacea) as bioindicator species in different aquatic habitats in the Bolu region, Turkey. Ecological Indicators 4, 139–147.
Lister, G.S., Kelts, K., Chen, K.Z., Yu, J.Q., Niessen, F., 1991. Lake Qinghai, China: closed-basin lake levels and the oxygen isotope record for ostracoda since the latest Pleistocene. Palaeogeography, Palaeoclimatology, Palaeoecology 84, 141–162.
Löffler, H., 1969. Recent and subfossil distribution of *Cytherissa lacustris* (Ostracoda) in lake Constance. Mitteilungen der Internationalen Vereinigung für theoretische und angewandte Limnologie 17, 240–251.
McGregor, D.L., 1969. The reproductive potential, life history and parasitism of the freshwater ostracod *Darwinula stevensoni* (Brady and Robertson). In: Neale, J.W. (Ed.), The Taxonomy, Morphology and Ecology of Recent Ostracoda. Proceedings of the 2nd International Symposium on Ostracoda, Edinburgh, pp. 194–221.
Meisch, C., 2000. Freshwater Ostracoda of Western and Central Europe. Spektrum, Heidelberg. 522 pp.
Mezquita, F., Roca, J.R., Reed, J.M., Wansard, G., 2005. Quantifying species–environment relationships in non-marine Ostracoda for ecological and palaeoecological studies: examples using Iberian data. Palaeogeography, Palaeoclimatology, Palaeoecology 225, 93–117.
Mischke, S., Wünnemann, B., 2006. The Holocene salinity history of Bosten Lake (Xinjiang, China) inferred from ostracod species assemblages and shell chemistry: possible palaeoclimatic implications. Quaternary International 154–155, 100–112.
Mischke, S., Herzschuh, U., Massmann, G., Zhang, C.J., 2007. An ostracod-conductivity transfer function for Tibetan lakes. Journal of Paleolimnology 38, 509–524.
Mischke, S., Kramer, M., Zhang, C.J., Shang, H.M., Herzschuh, U., Erzinger, J., 2008. Reduced early Holocene moisture availability in the Bayan Har Mountains, northeastern Tibetan Plateau, inferred from a multi-proxy lake record. Palaeogeography, Palaeoclimatology, Palaeoecology 267, 59–76.
Nakamura, T., Niu, E., Oda, H., Ikeda, A., Minami, M., Takahashi, H., Adachi, M., Pals, L., Gottdang, A., Suya, N., 2000. The HVEE Tandetron AMS system at Nagoya University. Nuclear Instruments and Methods in Physics Research B172, 52–57.
Nüchterlein, H., 1969. Süßwasserostracoden aus Franken. Ein Beitrag zur Systematik und Ökologie der Ostracoden. Internationale Revue der gesamten Hydrobiologie 54, 223–287.
Ranta, E., 1979. Population biology of *Darwinula stevensoni* (Crustacea, Ostracoda) in an oligotrophic lake. Annales Zoolo Fennici 16, 28–35.
Reimer, P.J., Baillie, M.G.L., Bard, E., Bayliss, A., Beck, J.W., Bertrand, C.J.H., Blackwell, P.G., Buck, C.E., Burr, G.S., Cutler, K.B., Damon, P.E., Edwards, R.L., Fairbanks, R.G., Friedrich, M., Guilderson, T.P., Hogg, A.G., Hughen, K.A., Kromer, B., McCormac, G., Manning, S., Bronk Ramsey, C., Reimer, R.W., Remmele, S., Southon, J.R., Stuiver, M., Talamo, S., Taylor, F.W., van der Plicht, J., Weyhenmeyer, C.E., 2004. Intcal04 terrestrial radiocarbon age calibration, 0–26 cal kyr BP. Radiocarbon 46, 1029–1058.
Ricketts, R.D., Johnson, T.C., Brown, E.T., Rasmussen, K.A., Romanovsky, V.V., 2001. The Holocene paleolimnology of Lake Issyk-Kul, Kyrgyzstan: trace element and stable isotope composition of ostracodes. Palaeogeography, Palaeoclimatology, Palaeoecology 176, 207–227.
Rieradevall, M., Roca, J.R., 1995. Distribution and population dynamics of ostracodes (Crustacea, Ostracoda) in a karstic lake: Lake Banyoles (Catalonia, Spain). Hydrobiologia 310, 189–196.
Stott, L., Cannariato, K., Thunell, R., Haug, G.H., Koutavas, A., Lund, S., 2004. Decline of surface temperature and salinity in the western tropical Pacific Ocean in the Holocene epoch. Nature 431, 56–59.
Talbot, M.R., 1990. A review of the palaeohydrological interpretation of carbon and oxygen isotopic ratios in primary lacustrine carbonates. Chemical Geology 80, 261–279.
Ter Braak, C.J.F., Šmilauer, P., 2002. CANOCO 4.5: Biometrics. Wageningen University and Research Center, Wageningen. 500 pp.
Van der Meeren, T., Almendinger, J.E., Ito, E., Martens, K., 2010. The ecology of ostracodes (Ostracoda, Crustacea) in western Mongolia. Hydrobiologia 641, 253–273.
Van Doninck, K., Schön, I., Martens, K., Goddeeris, B., 2003. The life-cycle of the asexual ostracod *Darwinula stevensoni* (Brady et Robertson, 1870) (Crustacea, Ostracoda) in a temporate pond. Hydrobiologia 500, 331–340.
Von Grafenstein, U., Erlenkeuser, H., Trimborn, P., 1999. Oxygen and carbon isotopes in modern fresh-water ostracod valves: assessing vital offsets and autecological effects of interest for palaeoclimate studies. Palaeogeography, Palaeoclimatology, Palaeoecology 148, 133–152.
Wang, S.M., Dou, H.S., 1998. Annals of Lakes in China. Science Press, Beijing. 580 pp. (in Chinese).
Wang, S.M., Ji, L., 1995. Paleolimnology of Hulun Lake. University of Science and Technology of China Press, Hefei. 125 pp. (in Chinese).
Wen, R.L., Xiao, J.L., Chang, Z.G., Zhai, D.Y., Xu, Q.H., Li, Y.C., Itoh, S., 2010a. Holocene precipitation and temperature variations in the East Asian monsoonal margin from pollen data from Hulun Lake in northeastern Inner Mongolia, China. Boreas 39, 262–272.
Wen, R.L., Xiao, J.L., Chang, Z.G., Zhai, D.Y., Xu, Q.H., Li, Y.C., Itoh, S., Lomtatidze, Z., 2010b. Holocene climate changes in the mid-high latitude monsoon margin reflected by the pollen record from Hulun Lake, northeastern Inner Mongolia. Quaternary Research 73, 293–303.
Wilkinson, I.P., Bubikyan, S.A., Gulakyan, S.Z., 2005. The impact of late Holocene environmental change on lacustrine Ostracoda in Armenia. Palaeogeography, Palaeoclimatology, Palaeoecology 225, 187–202.
Wrozyna, C., Frenzel, P., Steeb, P., Zhu, L.P., van Geldern, R., Mackensen, A., Schwalb, A., 2010. Stable isotope and ostracode species assemblage evidence for lake level changes of Nam Co, southern Tibet, during the past 600 years. Quaternary International 212, 2–13.
Xia, J., Haskell, B.J., Engstrom, D.R., Ito, E., 1997b. Holocene climate reconstructions from tandem trace-element and stable-isotope composition of ostracodes from Cold-water Lake, North Dakota, U.S.A. Journal of Paleolimnology 17, 85–100.
Xia, J., Ito, E., Engstrom, D.R., 1997a. Geochemistry of ostracode calcite: part 1, an experimental determination of oxygen isotope fractionation. Geochimica et Cosmochimica Acta 61, 377–382.
Xiao, J.L., Chang, Z.G., Wen, R.L., Zhai, D.Y., Itoh, S., Lomtatidze, Z., 2009. Holocene weak monsoon intervals indicated by low lake levels at Hulun Lake in the monsoonal margin region of northeastern Inner Mongolia, China. The Holocene 19, 899–908.
Xu, Z.J., Jiang, F.Y., Zhao, H.W., Zhang, Z.B., Sun, L., 1989. Annals of Hulun Lake. Jilin Literature and History Publishing House, Changchun. 691 pp. (in Chinese).
Zhai, D.Y., Xiao, J.L., Zhou, L., Wen, R.L., Chang, Z.G., Pang, Q.Q., 2010. Similar distribution pattern of different phenotypes of *Limnocythere inopinata* (Baird) in a brackish-water lake in Inner Mongolia. Hydrobiologia 651, 185–197.
Zhang, J.C., Lin, Z.G., 1985. Climate of China. Shanghai Scientific and Technical Publishers, Shanghai. 603 pp. (in Chinese).
Zhang, P.X., Zhang, B.Z., Yang, W.B., 1989. On the model of post-glacial palaeoclimatic fluctuation in Qinghai Lake region. Quaternary Sciences 1, 66–77 (in Chinese).